Proceedings of the 2003 IEEE/RSJ
Intl. Conference on Intelligent Robots and Systems
Las Vegas, Nevada · October 2003

ZMP Analysis for Arm/Leg Coordination

Kensuke Harada, Shuuji Kajita, Kenji Kaneko, and Hirohisa Hirukawa

National Institute of Advanced Industrial Science and Technology(AIST)
1-1-1 Umezono, Tsukuba 305-8568, JAPAN
{kensuke.harada, s.kajita, k.kaneko, hiro.hirukawa }@aist.go.jp

***Abstract*— This paper newly considers the ZMP(Zero Moment Point) of a humanoid robot under arm/leg coordination. By considering the infinitesimal displacement and the moment acting on the convex hull of the supporting points, we show that our method for determining the region of ZMP can be applicable to several cases of the arm/leg coordination tasks. We first express two kinds of ZMPs for such coordination tasks, i.e., the conventional ZMP, and the "Generalized Zero Moment Point (GZMP)" which is a generalization of the ZMP to the arm/leg coordination tasks. By projecting the edges of the convex hull of the supporting points onto the floor, we show that the position and the region of the GZMP for keeping the dynamical balance can be uniquely obtained. The effectiveness of the proposed method is shown by simulation results(see video).**

I. INTRODUCTION

Since the kinematical structure of a humanoid robot is similar to that of a human, a humanoid robot is expected to work instead of a human in the same environment. To accomplish the required tasks under such an environment, it should be considered that a humanoid robot touches an environment coordinating two arms and two legs.

The ZMP (Zero Moment Point) is defined to be a point on the ground at which the tangential component of the moment generated by the ground reaction force/moment becomes zero. For a humanoid robot whose hands do not touch an environment, a humanoid robot can walk on a flat ground with keeping the dynamical balance if the ZMP is included in the convex hull of the foot supporting area. On the other hand in this research, we analyze the ZMP for a humanoid robot whose hands touch an environment.

Now, let us consider what makes the ZMP analysis of the arm/leg coordination tasks difficult. Fig.1 shows two examples of the arm/leg coordination tasks where one of the two hands is touching an object. In Fig.1(a), a humanoid robot is walking on the ground with touching an object. Since the contact state changes frequently, it becomes difficult to plan the smooth trajectory of the desired ZMP between two different contact states. On the other hand, In Fig.(b), a humanoid robot pulls an object. In such a case, defining the region of the ZMP for keeping the dynamical balance is out of our intuition since the robot can keep the dynamical balance even if the ZMP is behind the foot supporting area.

Fig.1(c) shows the basic idea of the proposed method

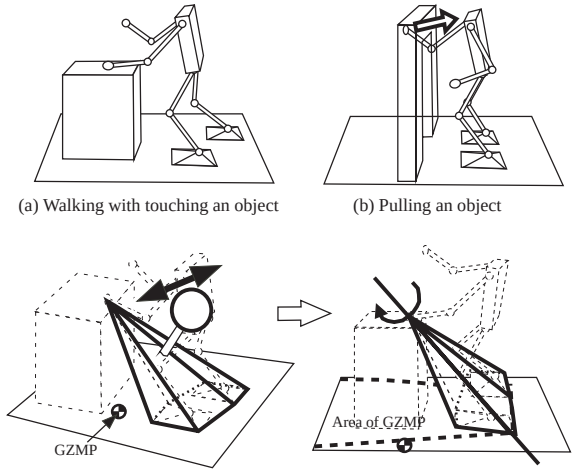

(a) Walking with touching an object (b) Pulling an object

(c) Explanation of the proposed method

Fig. 1. Arm/Leg Coordination by a Humanoid Robot

for defining the ZMP for arm/leg coordination tasks. Since a humanoid robot whose hands do not touch an environment can keep the dynamical balance if the ZMP is included in the convex hull of the foot supporting area, we define the convex hull of the supporting points including the contact points between the hands and the environment for the arm/leg coordinated tasks. For such arm/leg coordination, we use the same definition of ZMP as for a humanoid robot whose hands do not touch an environment, and name it as the "Generalized Zero Moment Point (GZMP)". Corresponding to the given motion of the robot, the GZMP is defined on the floor. If the GZMP is on the edge of an area defined in this paper, the robot will fall down by the moment around the edge of the convex hull. By using this approach, we show that the GZMP can be applied to several cases of the arm/leg coordination tasks. We also show that, by approximating the motion of a robot by the inverted pendulum, we can obtain the smooth trajectory of the GZMP even if there exists the change of contact states.

In this paper, after showing the relevant works, we state that there are two kinds of ZMPs for arm/leg coordination in Section 3. We then obtain the stable region of the GZMP in Section 4. To verify the effectiveness of our proposed method, simulation results are shown in Section 5.

II. Relevant Works

As for the arm/leg coordination of a humanoid robot, Inoue et al. [2] determined the posture of a humanoid robot taking the manipulability of the arms into consideration. Takenaka [10] proposed a method for modifying the posture of a humanoid robot according to the force applied by the hands.

As for the indices of a humanoid robot to keep the dynamical balance, Vukobratovic et al.[5] proposed the ZMP(Zero Moment Point). Goswami[6] proposed the FRI(Foot Rotation Indicator) where the robot will fall down if the FRI is out of the foot supporting area. For a quadruped robot to walk stably on a sloped surface, Yoneda et al.[7] and P.B. Wieber[8] studied the stability of the walking systems. Kitagawa et al. [9] proposed the "Enhanced ZMP" for the arm/leg coordination tasks for a humanoid robot.

However, there has been no research on the ZMP analysis of a humanoid robot which can take into account several cases of arm/leg coordination tasks as shown in Fig.1.

III. Two ZMPs

Fig. 2 shows the model of a humanoid robot used in this paper. We assume that the sole and the hand contact with the ground and the environment, respectively. Σ_R and Σ_i denote the reference coordinate and the coordinate frame fixed to the i-th $(i = 1, \cdots, n)$ link of the robot, respectively. $p_{Hj}(=[x_{Hj}\ y_{Hj}\ z_{Hj}]^T)$, $p_{Fj}(=[x_{Fj}\ y_{Fj}\ z_{Fj}]^T)$ $(j = 1,2)$, and $p_i(=[x_i\ y_i\ z_i]^T)$ denote the position vector of the contact point between the j-th hand and the object, a point included in the contact surface between the j-th foot and the ground, and the origin of Σ_i, respectively. m_i, I_i, and ω_i denote the mass, the inertia tensor and the angular velocity vector, respectively, of the link i. $p_G(=[x_G\ y_G\ z_G]^T)$ denotes the vector of the center of gravity of the robot defined by $p_G = \sum_{i=1}^n m_i p_i / \sum_{i=1}^n m_i$. $p_P(=[x_P\ y_P\ z_P]^T)$ and $p_E(=[x_E\ y_E\ z_E]^T)$ denote the position vectors of the zero moment point and the generalized zero moment point (GZMP), respectively. f_P and τ_P denote the ground reaction force/torque at the ZMP , and f_E and τ_E denote the reaction force/torque at the GZMP. For simplicity, we neglect the effect of internal force in this paper.

We first explain that there are two kinds of ZMPs in the arm/leg coordination tasks. Since the (conventional) ZMP is the center of pressure of the foot supporting area [6], we need to consider all the sources of the force/moment acting in the foot supporting area. When the hands of a humanoid robot contact with an environment, the sources of the force/moment acting in the foot supporting area are the inertial force of the robot, gravity force, and the hand reaction force. Therefore, the ZMP for the arm/leg coordination is redefined as follows:

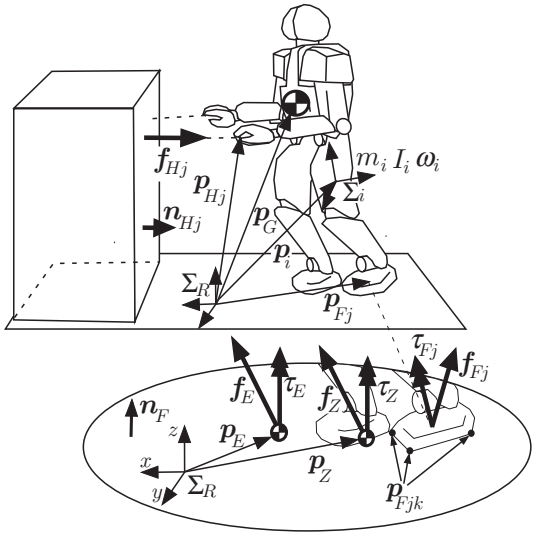

Fig. 2. Model of the System

Definition 1 (Zero Moment Point)
The zero moment point (ZMP) is the point on the ground at which the moment $\tau_P = [\tau_{Px}\ \tau_{Py}\ \tau_{Pz}]^T$ *generated by the reaction force and the reaction moment satisfies* $\tau_{Px} = \tau_{Py} = 0$*, where the reaction force and moment is generated by the inertial force, the gravity force, and the hand reaction force.*

This is the redefinition of the conventional ZMP[5], and Takenaka[11] also considered the same definition of the ZMP for the arm/leg coordination tasks. The reaction force/moment at the ZMP can be formulated as

$$f_P = M(\ddot{p}_G - g) - \sum_{j=1}^{2} f_{Hj}, \tag{1}$$

$$= \sum_{j=1}^{2} f_{Fj}, \tag{2}$$

$$\tau_P = \dot{L}_G + M(p_G - p_P) \times (\ddot{p}_G - g) - \sum_{j=1}^{2} (p_{Hj} - p_P) \times f_{Hj}, \tag{3}$$

$$= \sum_{j=1}^{2} \{(p_{Fj} - p_P) \times f_{Fj} + \tau_{Fj}\}, \tag{4}$$

where $M = \sum_{i=1}^n m_i$, $g = [0\ \ 0\ \ -g]^T$, and $L_G(=[L_{Gx}\ L_{Gy}\ L_{Gz}]^T)$ denote the mass of the object, gravity vector, and the angular momentum about the center of mass defined by

$$L_G = \sum_{i=1}^{n} \{m_i(p_i - p_G) \times \dot{p}_i + I_i \omega_i\}, \tag{5}$$

respectively. Substituting $\tau_{Px} = \tau_{Py} = 0$ into eq.(3) and solving with respect to p_P, the position of the ZMP can be obtained by

$$x_P = \frac{-\dot{L}_{Gy} + Mx_G(\ddot{z}_G + g) - M(z_G - z_P)\ddot{x}_G}{M(\ddot{z}_G + g) - \sum_{j=1}^{2} f_{Hjz}} - \frac{\sum_{j=1}^{2}\{x_{Hj} f_{Hjz} - (z_{Hj} - z_Z) f_{Hjx}\}}{M(\ddot{z}_G + g) - \sum_{j=1}^{2} f_{Hjz}}, \quad (6)$$

$$y_P = \frac{\dot{L}_{Gx} + My_G(\ddot{z}_G + g) - M(z_G - z_P)\ddot{y}_G}{M(\ddot{z}_G + g) - \sum_{j=1}^{2} f_{Hjz}} - \frac{\sum_{j=1}^{2}\{y_{Hj} f_{Hjz} - (z_{Hj} - z_P) f_{Hjy}\}}{M(\ddot{z}_G + g) - \sum_{j=1}^{2} f_{Hjz}}. \quad (7)$$

Here, in this definition of the ZMP, since the force/moment acting on the ZMP (f_P,m_P) might balance with the hand reaction force(f_{Hj}), we can see that the robot does not always fall down even if the ZMP is on the edge of the foot supporting area. To generalize the ZMP to the arm/leg coordination tasks, we define the following ZMP

Definition 2 (Generalized Zero Moment Point)
The generalized zero moment point (GZMP) is the point on the floor at which the moment $\tau_E = [\tau_{Ex} \ \tau_{Ey} \ \tau_{Ez}]^T$ *generated by the reaction force and the reaction moment satisfies* $\tau_{Ex} = \tau_{Ey} = 0$*, where the reaction force and moment is generated by the inertial force and the gravity force.*

The definition of the GZMP is same as the definition of the ZMP for a humanoid robot whose hands do not touch an environment. The force (f_E) and the moment (τ_E) at the GZMP are expressed as follows:

$$f_E = M(\ddot{p}_G - g) \quad (8)$$

$$= \sum_{j=1}^{2}(f_{Hj} + f_{Fj}), \quad (9)$$

$$\tau_E = \dot{L}_G + M(p_G - p_E) \times (\ddot{p}_G - g) \quad (10)$$

$$= \sum_{j=1}^{2}\{(p_{Hj} - p_E) \times f_{Hj} + (p_{Fj} - p_E) \times f_{Fj} + \tau_{Fj}\}. \quad (11)$$

The position of the GZMP can be obtained by substituting $\tau_{Ex} = \tau_{Ey} = 0$ into eq.(10) and solving with respect to p_E:

$$x_E = \frac{-\dot{L}_{Gy} + Mx_G(\ddot{z}_G + g) - M(z_G - z_E)\ddot{x}_G}{M(\ddot{z}_G + g)}, \quad (12)$$

$$y_E = \frac{\dot{L}_{Gx} + My_G(\ddot{z}_G + g) - M(z_G - z_E)\ddot{y}_G}{M(\ddot{z}_G + g)}. \quad (13)$$

Eqs.(12) and (13) are same as those for a humanoid robot whose hands do not touch an environment. Since the position of the GZMP is defined only by the inertial and the gravity force, the robot will fall down if the position of the GZMP is on the edge of the region defined in the next section.

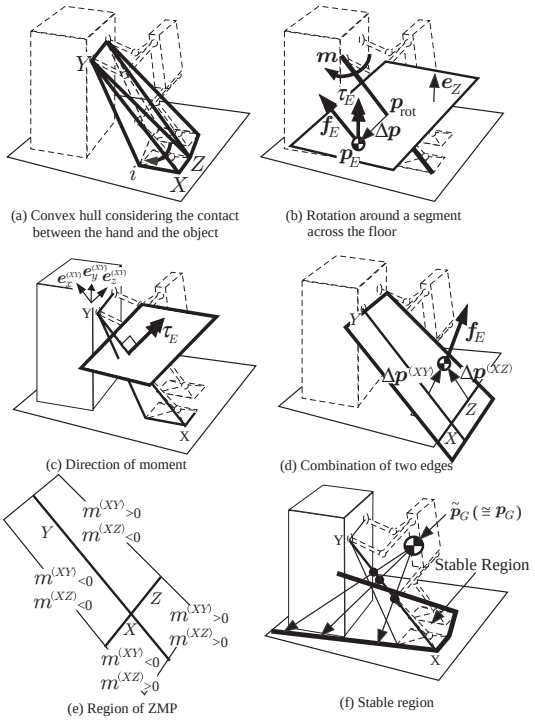

Fig. 3. Explanation of the proposed method

IV. Region of GZMP

A. Convex Hull

For a humanoid robot whose hands do not touch an environment, the robot can keep the dynamical balance if the ZMP is included in the convex hull of the foot supporting area. By extending this idea, we define the convex hull of the supporting points including the contact points between the hands and the environment(Fig.3(a)). While there are many edges included in the convex hull, we extract the edges of the convex hull where a robot might fall down by the moment around the edge.

As shown in Fig.3(a), we focus on three vertices j, X, and Y included in the convex hull. Since the vertex j can leave from the environment while it cannot go inside of the environment, the following inequality can be satisfied:

$$d_j^{(XY)} \Delta q_{\rm rot} \geq 0, \quad (j = 1, \cdots, L), \quad (14)$$

where

$$d_j^{(XY)} = \begin{bmatrix} n_j \\ (p_j - p_{\rm rot}) \times n_j \end{bmatrix}^T,$$

$$\Delta q_{\rm rot} = \left[\Delta p_{\rm rot}^T \ \ \Delta\theta_{\rm rot}^T\right]^T,$$

$p_{\rm rot}$, $\Delta\theta_{\rm rot}$, and n_j denote the position vector of a point included in the edge formed by the vertices X and Y, the infinitesimal rotational displacement of the convex hull around $p_{\rm rot}$, and the unit normal vector of the environment where the vertex j contacts, respectively. We consider

rotating the convex hull around the edge formed by the vertices X and Y as

$$\Delta p_{\rm rot} = 0, \tag{15}$$

$$\Delta\theta_{\rm rot} = \frac{p_X - p_Y}{\| p_X - p_Y \|}\Delta\theta, \tag{16}$$

where $\Delta\theta$ denotes the rotation angle of the convex hull. Substituting eqs.(15) and (16) into ineq.(14) and aggregating for all the vertices contacting with the environment except for X and Y, we obtain the following inequality:

$$d^{(XY)}\Delta\theta > 0, \tag{17}$$

where

$$d^{(XY)} = \begin{bmatrix} \{(p_1 - p_{\rm rot})\times n_1\}^T \\ \vdots \\ \{(p_L - p_{\rm rot})\times n_L\}^T \end{bmatrix} \frac{p_X - p_Y}{\| p_X - p_Y \|}.$$

By using ineq.(17), we can obtain the following proposition:

Proposition 1 (Feasible Edge of the Convex Hull)
If all the elements of $d^{(XY)}$ in ineq.(17) is positive or negative, the convex hull can rotate around the edge formed by the vertices X and Y in the direction of $\Delta\theta > 0$ or $\Delta\theta < 0$, respectively.

If the convex hull can rotate around the edge, there is a possibility where the robot might fall down.

B. Moment around the Edge

Next, we focus on the moment around the edge of the convex hull. By using the duality between the force and the infinitesimal displacement, the moment around the edge including the vertices X and Y should satisfy the following equation:

$$m^{(XY)} = d^{(XY)T}k, \quad k \geq 0. \tag{18}$$

If Proposition 2 is satisfied, eq.(18) can shows us that the direction of moment around the edge is same as the direction of $\Delta\theta$.

Then we consider the virtual floor above the real floor as shown in Fig.3(b). By using the force f_E and moment m_E at the GZMP on the virtual floor, we can formulate the moment around the edge including the vertices X and Y as

$$m^{(XY)} = \frac{p_X^T - p_Y^T}{\| p_X - p_Y \|}((p_E - p_{\rm rot})\times f_E + e_Z e_Z^T \tau_E), \tag{19}$$

where e_Z denotes the unit normal vector of the virtual floor. From eq.(19), we can see that τ_E affects the moment around the edge when $(p_X - p_Y)^T e_Z \neq 0$. In this case, we cannot judge the moment around the edge by simply considering the relationship of position between the edge and the GZMP. Thus we redefine the GZMP as follows (Fig.3(c)):

Definition 3 (GZMP(Modified))
The (modified) generalized zero moment point $p_E^{(XY)} = [x_E^{(XY)}\ y_E^{(XY)}\ z_E^{(XY)}]^T$ is the point on the (virtual) floor at which the moment τ_E generated by the reaction force and the reaction moment becomes normal to the edge of the convex hull satisfying the Proposition 2.

By using this definition, we can consider the direction of moment around the edge by considering the position of the GZMP. Let the unit vector of the direction of τ_E be $e_z^{(XY)}$, and two unit vectors normal to $e_z^{(XY)}$ be $e_x^{(XY)}$ and $e_y^{(XY)}$. The position of the GZMP modified in Definition 3 can be expressed as

$$\begin{bmatrix} x_E^{(XY)} \\ y_E^{(XY)} \end{bmatrix} = -\{ME[(\ddot{p}_G - g)\times]D\}^{-1} \{ME(p_G - ez_E^{(XY)})\times(\ddot{p}_G - g) + E\dot{L}_G\}, \tag{20}$$

where $E = [e_x^{(XY)}\ \ e_y^{(XY)}]^T$, $D = \begin{bmatrix} 1 & 0 & 0 \\ 0 & 1 & 0 \end{bmatrix}^T$, $e = [0\ 0\ 1]^T$.

Since the direction of moment around the edge satisfying Proposition 1 is limited by eq.(18), the region of the GZMP is also limited. To see the region of the GZMP, we consider the combination of two edges sharing a common vertex as shown in Fig.3(d). We consider the GZMP on the plane including two edges sharing a common vertex. By using two edges, we can divide the plane into four regions. These regions can be identified by the direction of moment around the edge defined by eq.(19). The region of the GZMP is limited to one of the four regions by using eq.(18) if both of the edges satisfy Proposition 2. Fig.3(d) shows the region of the GZMP corresponding to $m^{(XY)} > 0$ and $m^{(XZ)} < 0$. Also, Fig.3(e) shows four regions on the plane defined by the vertices X, Y, and Z.

We further consider the change of moment when the robot begins to roll around the edge. Since the moment around the edge generated by the inertial force does not change even if the convex hull rotates around the edge, we only consider the moment generated by the gravity force. The change of moment is expressed as:

$$\begin{aligned} &\Delta m^{(XY)} \\ &= -M\frac{p_X^T - p_Y^T}{\| p_X - p_Y \|}(p_G - p_{\rm rot})\times\{(R_{-\Delta\theta} - I_3)g\} \\ &= M\frac{p_X^T - p_Y^T}{\| p_X - p_Y \|^2}(p_G - p_{\rm rot})\times\{(p_X - p_Y)\times g\}\Delta\theta \\ &\triangleq L^{(XY)}\Delta\theta \end{aligned} \tag{21}$$

where $R_{-\Delta\theta}$ denotes the rotation matrix around the edge including the vertices X and Y whose amount of rotation is $-\Delta\theta$, and I_3 denotes the 3×3 identity matrix. Since the sign of $\Delta\theta$ is same as that of $m^{(XY)}$ for the edges satisfying Proposition 1, the robot will be accelerated when the convex hull begins to roll if the sign of $\Delta m^{(XY)}$ is different from that of $\Delta\theta$. Therefore, we can introduce the following Proposition:

Proposition 2 (Change of Moment around the Edge)
For an edge of the convex hull satisfying Proposition 1, the angular velocity will increase when the convex hull begins to roll, if $L^{(XY)} < 0$ is satisfied.

Later, we will show an example where the robot will not fall down even if the GZMP is on the edge of the area by using this Proposition.

C. Projection

To obtain the region of the GZMP on the floor, we consider the method for projecting the edges of the convex hull onto the floor. We first introduce a vector $\tilde{p}_G(=[\tilde{x}_G \;\; \tilde{y}_G \;\; \tilde{z}_G]^T)$ and consider the change of coordinates between p_G and $\tilde{p}_G$ defined by

$$\begin{aligned} -\dot{L}_{Gy}/M + x_G(\ddot{z}_G+g) - (z_G - z_E)\ddot{x}_G & \\ = \tilde{x}_G(\ddot{\tilde{z}}_G+g) - (\tilde{z}_G - z_E)\ddot{\tilde{x}}_G, & \quad (22)\\ \dot{L}_{Gx}/M + y_G(\ddot{z}_G+g) - (z_G - z_E)\ddot{y}_G & \\ = \tilde{y}_G(\ddot{\tilde{z}}_G+g) - (\tilde{z}_G - z_E)\ddot{\tilde{y}}_G, & \quad (23)\\ \tilde{z}_G = z_G. & \quad (24) \end{aligned}$$

Applying the change of coordinates to eqs.(12) and (13), the position of the GZMP can be defined as follows:

$$x_E = \frac{\tilde{x}_G(\ddot{\tilde{z}}_G+g) - (\tilde{z}_G - z_E)\ddot{\tilde{x}}_G}{\ddot{\tilde{z}}_G+g}, \quad (25)$$

$$y_E = \frac{\tilde{y}_G(\ddot{\tilde{z}}_G+g) - (\tilde{z}_G - z_E)\ddot{\tilde{y}}_G}{\ddot{\tilde{z}}_G+g}. \quad (26)$$

We note that eqs.(25) and (26) are same as those of an inverted pendulum. Assume that the real floor is the $x_E - y_E$ plane when $z_E = 0$. As shown in Fig.4, the following proposition can be hold for the projection of the GZMP included in a virtual floor above the real one:

Proposition 3 (Projection of GZMP)
Draw a line including both of $\tilde{p}_G(z_E = z_G)$ and the GZMP on the virtual floor. The intersection of the line and the ground corresponds to the GZMP on the real ground.

Proof *In eqs.(25) and (26), the GZMP is concentrated on a sigle point:*

$$\tilde{p}_G(z_E = z_G) = \begin{bmatrix} x_G - \dot{L}_{Gy}/(M(\ddot{z}_G+g)) \\ y_G + \dot{L}_{Gx}/(M(\ddot{z}_G+g)) \\ z_G \end{bmatrix} \quad (27)$$

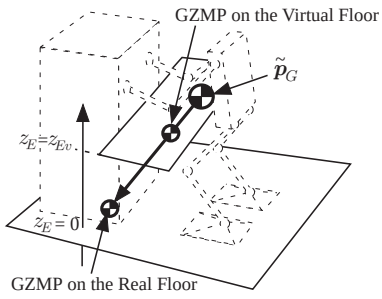

Fig. 4. Projection of the Generalized Zero Moment Point

when $z_E = \tilde{z}_G$. Moreover, eqs.(25) and (26) are linear equations with respect to p_E. Therefore, since all points on the line including both $\tilde{p}_G(z_E = z_G)$ and the GZMP on the virtual floor can be the GZMP, we confirm the theorem is correct.

By using this Proposition, we project the edges of the convex hull onto the floor.

Now, we summarize the method for obtaining the the region of the GZMP for keeping the dynamical balance of a humanoid robot is summarized by the following theorem:

Theorem 1 (Region of GZMP)
Project the edges of the convex hull satisfying Proposition 1 onto the ground by using Proposition 3 as shown in Fig.3(f). The region of the GZMP is defined by considering the direction of moment using eq.(18). If Proposition 2 is satisfied, the robot might fall down by the moment around the edge.

D. Approximation by the Inverted Pendulum

For biped robots including humanoid robots, the motion of the robot is often approximated the linear inverted pendulum mode[3], [4]. By using the approximation by the inverted pendulum, there are a couple of merits shown in the following:

1) Since the ground reaction torque around the fulcrum of a inverted pendulum is 0, $\tau_E \cong 0$ is satisfied if the motion of a humanoid robot is well approximated by the inverted pendulum. Since the definition of the GZMP does not depend on the direction of moment τ_E, the position of the GZMP does not change even if the definition of the GZMP is modified by Definition 3 and $p_E^{(XY)} \cong p_E$ is satisfied. In this case, we can obtain the smooth trajectory of the GZMP even if the contact states change frequently.
2) We defined the change of coordinates in eqs.(22) and (23) between p_G and $\tilde{p}_G$. If the motion of a humanoid robot is approximated by the inverted

pendulum, $\dot{L}_G \cong 0$ is satisfied which means $p_G \cong \tilde{p}_G$. By using this approximation, we do not need the change of coordinates.

V. Simulation

We first consider the convex hull shown in Fig. 5. In both cases shown in Fig.5, the face of the convex hull formed by the vertices A, B, C, and D can be regarded as the foot supporting area, and the vertex E can be regarded as the contact point between the hand and the environment. The difference between (a) and (b) is the direction of the unit normal vector of the environment.

By calculating $d^{(XY)}$, the convex hull shown in Fig.5(a) might rotate around the edges BC, CD, DE, and EB, and cannot rotate around the edges AD, AE, AB, and CE. On the other hand, the convex hull shown in Fig.5(b) might rotate around the edges AB, BE, BC, and DE, and cannot rotate around the edges CD, AD, AE, and CE. Setting $p_G = [0\ 0\ 2]^T$, $\ddot{p}_G = [1\ 1\ 0]^T$, and $\dot{L}_G = 0$, the result of calculation of the projection of the edges onto the ground is shown in Fig.5(c) and (d).

Next, we consider two examples as shown in Fig.6. Fig.6(a) can be regarded as the case where the hand of a humanoid robot pulls the object, while Fig.6(b) can be regarded as the case of pushing an object. The difference between (a) and (b) is the direction of the normal vector of the object contacting with the hand. Since the direction of moment around the edge $m^{(BC)}$ becomes different, the region of the GZMP can be obtained as shown in the figure.

We further consider the examples shown in Fig.7. The position of the center of gravity is different between these two examples. Especially, in the example shown in Fig.7(b), since the sign of the change of the moment is same as the sign of $\Delta\theta$, we can see that the robot does not always fall down even if the GZMP is on the edge of the region.

Then we performed the simulation of an arm/leg coordination task by a humanoid robot. Consider the case where both hands of a humanoid robot touch the table. If one of the two hands is left from the table, the humanoid robot might lose the dynamical balance and fall down. Therefore, we have to first control the GZMP to be included in the region obtained by the convex hull formed by the other one of the two hands and both of the feet.

As a simulation software, we used the OpenHRP [12], [13]. The result of simulation is shown in Fig. 8. In the simulation, the body of the robot moves in the left side, and the GZMP is finally included into the region of the GZMP obtained by the convex hull formed by the left hand and both of the feet. The trajectory of the GZMP and the region of it are shown in Fig.9. The GZMP is calculated using the approximation by the inverted pendulum. As shown in the figure, the continuous trajectory of the

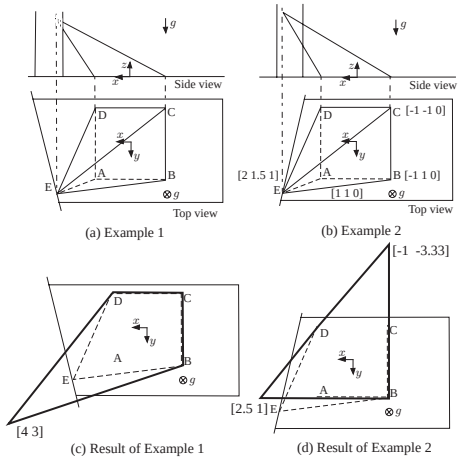

(a) Example 1 (b) Example 2

(c) Result of Example 1 (d) Result of Example 2

Fig. 5. Numerical Examples 1 and 2

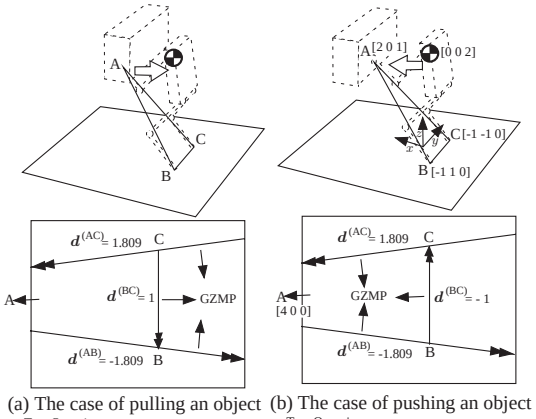

(a) The case of pulling an object (b) The case of pushing an object

Top: Overview
Bottom: Direction of moment (Double Arrow)
Region of GZMP (Single Arrow)

Fig. 6. Numerical Examples 3 and 4

GZMP is obtained taking the change of contact states into consideration.

On the other hand, in the simulation result shown in Fig.10, the right hand is left from the table without controlling the position of the body. As shown in the figure, the robot falls down.

VI. Conclusion

In this paper, we discussed the ZMP of a humanoid robot whose hands touch an environment. We generalized the ZMP to several cases of arm/leg coordination tasks such as the task of pulling an object, and the task with the change of contact states. The effectiveness of the proposed method is confirmed by simulation results. Experimental validation of the proposed method is considered to be our future research topic.

Finally, we would like to express our sincere gratitude to Dr. Kazuhito Yokoi, Dr. Fumio Kanehiro, and Mr. Kiyoshi Fujiwara who are the members of the humanoid research group for their helpful discussions.

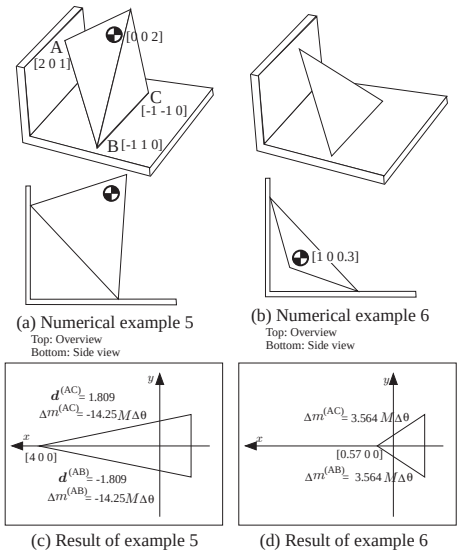

Fig. 7. Numerical Examples 5 and 6

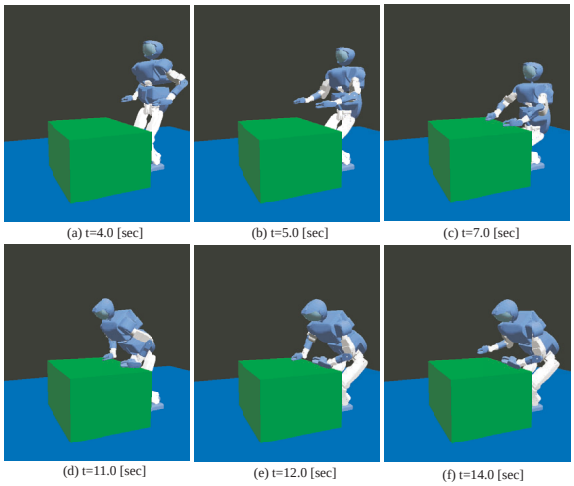

Fig. 8. Result of simulation 1

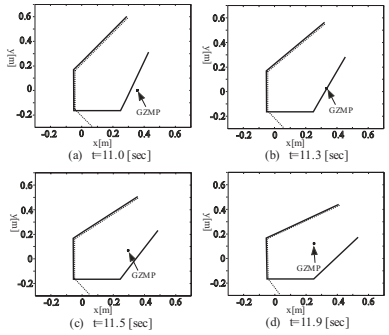

Fig. 9. GZMP and its stable region

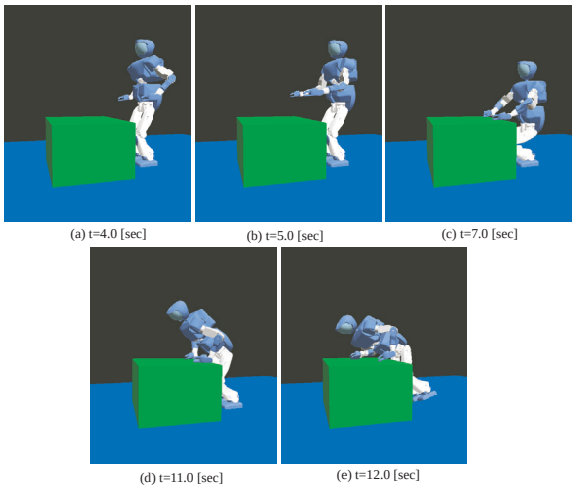

Fig. 10. Result of simulation 2

VII. REFERENCES

[1] K. Kaneko et al.: "Design of Prototype Humanoid Robotics Platform for HRP", Proc. of IEEE/RSJ Int. Conf. Intelligent Robots and Systems, 2002.

[2] K. Inoue, H. Yoshida, T. Arai, and Y. Mae: "Mobile Manipulation of Humanoids –Real-Time Control Based on Manipulability and Stability–", Proc. of IEEE Int. Conf. on Robotics and Automation, pp. 2217-2222, 2000.

[3] S. Kajita, T. Yamaura, and A. Kobayashi: "Dynamic Walking Control of a Biped Robot Along a Potential Energy Conserving Orbit", IEEE Trans. on Robotics and Automation, vol. 8, no. 4, pp. 431-438, 1992.

[4] S. Kajita, O. Matsumoto, and M. Saigo: "Real-time 3D Walking Pattern Generation for a Biped Robot with Telescopic Legs", Proc. of 2001 IEEE Int. Conf. on Robotics and Automation, pp. 2299-2036, 2001.

[5] M. Vukobratovic and J. Stepanenko: "On the Stability of Anthropomorphic Systems", Mathematical Biosciences, vol. 15, pp. 1-37, 1972.

[6] A. Goswami: "Postural Stability of Biped Robots and the Foot Rotation Indicator(FRI) Point", Int. J. of Robotics Research, vol. 19, no. 6, pp. 523-533, 1999.

[7] K. Yoneda S. Hirose: "Tumble Stability Criterion of Integrated Locomotion and Manipulation", Proc. of IEEE/RSJ Int. Conf. on Intelligent Robots and Systems, pp.870-876, 1996.

[8] P.-B. Wieber: "On the Stability of Walking Systems", Proc. of the Third IARP Int. Workshop on Humanoid and Human Friendly Robotics, pp.53-59, 2002.

[9] T. Kitagawa, K. Nagasaka, K. Nishiwaki, M. Inaba, and H. Inoue: "Generation of Stand-up-motion with Genetic Algorithm for a Humanoid", Proc. of the 17th Annual Conf. of RSJ, pp. 1191-1192, 1999.

[10] Takenaka: "Walking Pattern Generation for a Legged Mobile Robot", Japanese Patent, 3132156, 2001.

[11] Takenaka: "Posture Control for a Legged Mobile Robot", Japanese Patent Application, H10-230485, 1998.

[12] F. Kanehiro et al.: "Virtual humanoid robot platform to develop controllers of real humanoid robots without porting", Proc. of IEEE/RSJ Int. Conf. on Intelligent Robots and Systems, 2001.

[13] H. Hirukawa et al.: "OpenHRP: Open Architecture Humanoid Robot Platform", Proc. of Int. Symp. on Robotics Research, 2001.